Tolerance of Topological Surface States towards Magnetic Moments: Fe on Bi_2Se_3

M. R. Scholz,[1] J. Sánchez-Barriga,[1] D. Marchenko,[1] A. Varykhalov,[1] A. Volykhov,[2] L. V. Yashina,[2] and O. Rader[1]

[1]*Helmholtz-Zentrum Berlin für Materialien und Energie, Elektronenspeicherring BESSY II, Albert-Einstein-Strasse 15, D-12489 Berlin, Germany*

[2]*Department of Chemistry, Moscow State University, Leninskie Gory, 1/3, 119992 Moscow, Russia*

(Received 10 December 2011; published 22 June 2012)

We study the effect of Fe impurities deposited on the surface of the topological insulator Bi_2Se_3 by means of core-level and angle-resolved photoelectron spectroscopy. The topological surface state reveals surface electron doping when the Fe is deposited at room temperature and hole doping with increased linearity when deposited at low temperature (~ 8 K). We show that in both cases the surface state remains intact and gapless, in contradiction to current belief. Our results suggest that the surface state can very well exist at functional interfaces with ferromagnets in future devices.

DOI: 10.1103/PhysRevLett.108.256810 PACS numbers: 73.20.At, 71.70.Ej, 79.60.Dp

In contrast to ordinary insulators, the bulk band gap of a topological insulator [1–7] owes its existence to band inversion and strong spin-orbit coupling. Its surface is metallic due to spin-polarized surface states [4–7] where the spin is such that surface-state electrons that propagate in opposite directions carry opposite spins $\uparrow$ and $\downarrow$. This chirality is caused by time-reversal symmetry, and it prevents electron backscattering by 180°. The surface state itself and the topology of its band dispersion $E(k)$ enjoy protection by time-reversal symmetry against distortions such as surface impurities [4–7].

A magnetic field, on the other hand, breaks time-reversal symmetry, and the lifting of the Kramers degeneracy $E(k,\uparrow) = E(-k,\downarrow)$ causes a gap in the topological surface state at zero momentum (wave vector $k = 0$). This has been proven in transport measurements by applying 14 mT to a HgTe-based two-dimensional quantum spin Hall system [8]. For a three-dimensional topological insulator, much more efficient than using an external field is the exchange field from a deposited ferromagnet. For such a configuration, numerous electronic and spin effects have been predicted [9–17], among them the quantized topological magnetoelectric effect leading to half-integer charges at magnetic domain boundaries [9,10], a magnetoresistance increasing for parallel (sic) domain magnetizations [11], and an inverse spin-galvanic effect enabling the dissipationless magnetization reversal by an applied electric current [12].

While these effects are awaiting experimental verification, much progress has recently been made in the identification of appropriate three-dimensional topological insulator materials, starting with $Bi_{0.9}Sb_{0.1}$ [18]. The second generation of three-dimensional topological insulators, Bi_2Se_3 and Bi_2Te_3 [19–21], forms particularly simple systems, with the topological surface state appearing as a single Dirac cone at the $\bar{\Gamma}$ point of the surface Brillouin zone (i.e., where the two-dimensional electron wave vector $\mathbf{k}_\parallel$ is zero) and having a substantial spin polarization [19,22,23]. The band gaps are large enough to allow for room-temperature applications, but as-grown samples show a tendency for defects, such as Se vacancies and antisite defects, which lead to an n-type bulk doping (electron doping) so large that the samples are rendered metallic in their bulk.

Several studies have investigated the effect of magnetic moments on the topological surface state. When Bi_2Se_3 is doped with Fe in the bulk, a gap opens in the surface-state dispersion at Fe concentrations (melt composition relative to Bi) from 5% to 25% [24]. This includes concentrations for which the system remains paramagnetic down to low temperatures ($T = 2$ K), such as 12% Fe, where the surface-state band gap amounts to 45 meV [24]. When Bi_2Se_3 is p-doped (hole doped) in the bulk by Mn, it is possible to move the Fermi level into the bulk band gap [24]. Bulk Mn doping of Bi_2Te_3 has led to ferromagnetic order below temperatures of 12 K [25]. Unfortunately, photoemission of the Dirac point region remained inconclusive for these systems, possibly due to the strong p doping [25].

Most recently, Fe deposited directly on the surface of Bi_2Se_3 has been studied by means of angle-resolved photoemission [26]. It was revealed that the Fe dopes the surface substantially by electrons beyond its self-doping and opens at submonolayer coverages a band gap in the surface state of 100 meV. The authors assign this to the effect of the magnetic moment. They further speculate that this gap confirms the theoretical prediction [27] that the topological surface state mediates an out-of-plane anisotropy of the Fe magnetic moments without long-range ferromagnetic order [26].

In the present Letter, we investigate the behavior of Bi_2Se_3 upon Fe deposition. We characterize the system systematically by angle-resolved photoemission of the valence band and by photoemission of the Bi5d and Se3d core levels. In qualitative agreement with previous work [26], we observe energy shifts of the surface band structure consistent with electron doping if Fe is deposited on the

sample surface at room temperature. We find that the Dirac point cannot be shifted by more than ~150 meV. This saturation value is, however, less than half of what was reported previously [26]. Unfortunately, only the measurement temperature of 10–15 K but not the temperature of the sample during deposition was given in Ref. [26], so that we repeated our experiment for different deposition conditions. Interestingly, we find that the Dirac point shifts oppositely, i.e., consistently with hole doping, if the sample is cooled to low temperatures prior to Fe deposition. Most strikingly, we show direct evidence that the Dirac crossing point remains intact independently of the sample temperature and even under heavy Fe deposition. In fact, in no stage of Fe deposition does a band gap open in the topological surface state.

Single crystals of Bi_2Se_3 were grown by the Bridgman method and cleaved *in situ* with the sample kept at room temperature as well as at 8 K. The high quality of the achieved (111) surfaces is verified by the sharp features in angle-resolved photoemission of the valence band. Measurements have been carried out in ultrahigh vacuum of 1×10^{-10} mbar with a Scienta R8000 electron analyzer at the UE112-PGM2a beam line of BESSY II with *p*-polarized undulator radiation. Fe was deposited *in situ* from an e^--beam oven with the sample kept at the cleavage temperature, i.e., room temperature or 8 K. The evaporation rate has been repeatedly calibrated with a quartz microbalance and was typically 0.05 monoatomic layers (ML) per minute. Faster and slower depositions did not show any influence on the results.

We monitor the evolution of the topological surface-state band structure at room temperature after each deposition step of Fe. Figure 1 shows the $E(\mathbf{k}_\parallel)$ dispersion relations of the topological surface state measured along the $\bar{K}$-$\bar{\Gamma}$-$\bar{K}$ direction of the surface Brillouin zone. 18 eV photons have been used, which leads to a high contrast between bulk and surface states. The band structure undergoes a shift consistent with *n*-type surface doping (i.e., electron doping). The region of the bulk conduction band, situated in between the two branches of the topological surface state, alters in a peculiar way. At 0.1 ML Fe, the Dirac point has shifted by $\Delta E_D = 105$ meV relative to the pristine sample. More importantly, in our case, the shift saturates at $\Delta E_D = 150$ meV and 0.3 ML, considerably less than the $\Delta E_D > 300$ meV shift measured previously at a similar coverage [26].

To investigate the effect of the Fe adatoms on the surface electronic structure at higher energy resolution and to enable the suggested out-of-plane alignment of Fe moments mediated at low temperatures by the topological surface state [26], we cooled the Bi_2Se_3 sample down to 8 K after having deposited the Fe at room temperature [Figs. 2(a) and 2(b)]. Thus, for Bi_2Se_3, we are well below the recently suggested transition temperature of 30 K [28] and below the measurement temperature of 10–15 K of Ref. [26]. We find that, upon cooling, the Dirac point shifts to larger binding energies between 50 and 100 meV even for pristine Bi_2Se_3 samples [see Fig. 3(a)]. This effect is also visible in the core-level spectra and may be due to temporary residual gas adsorption, especially as it reverses after warming up. It is clearly seen in Figs. 2(a) and 2(b) that the Dirac point remains intact after Fe deposition. We are able to resolve a pair of M-shaped bands around 0.7 eV binding energy which are well-separated from the Dirac point. No gap has opened at the Dirac point. As pointed out above, at this coverage of 0.3 ML Fe, our samples are already in a saturated regime regarding the shift of the Dirac point towards a higher binding energy. Up to this stage of doping, our results are in agreement with those reported recently [26]. While the authors in Ref. [26] report an ongoing shift of the Dirac point, we do not observe any further shift up to an Fe thickness where the limit of detectability of the topological surface state is reached.

In order to clarify the reasons for the discrepancies, we reconsider at first the theoretical basis for the band gap in the topological surface state. The interaction which is expected to magnetize the impurities ferromagnetically out of plane is unanimously based on the assumption that the Dirac point is near the Fermi level [27–29], which is clearly not the case here and in Ref. [26].

Second, we consider the assignment of features to bulk- and surface-derived electronic bands. The upper M-shaped band at $\bar{\Gamma}$ has been taken for the bottom of the gap in

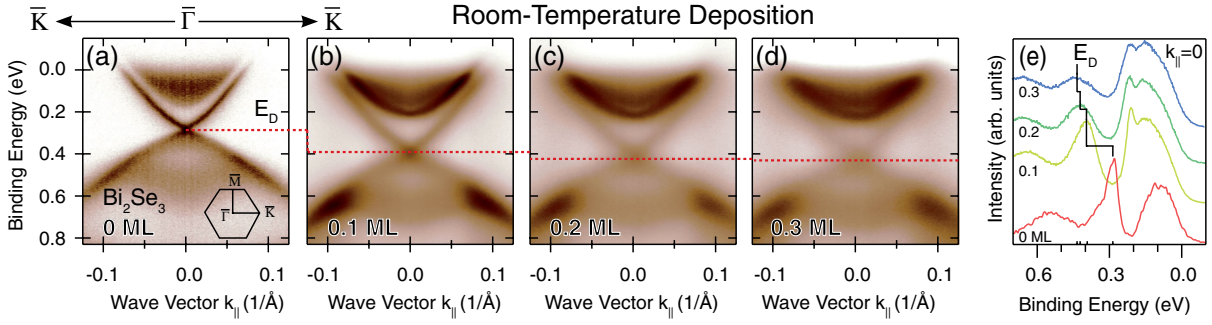

FIG. 1 (color online). Behavior of topological surface states upon deposition of Fe. Angle-resolved photoemission data at room temperature for Bi_2Se_3. The red dashed line follows the *n*-type (electron) surface-doping effect on the Dirac point (E_D). The Dirac point is clearly observed, and saturation of the surface-doping effect is seen at 0.3 ML Fe. The photon energy is 18 eV.

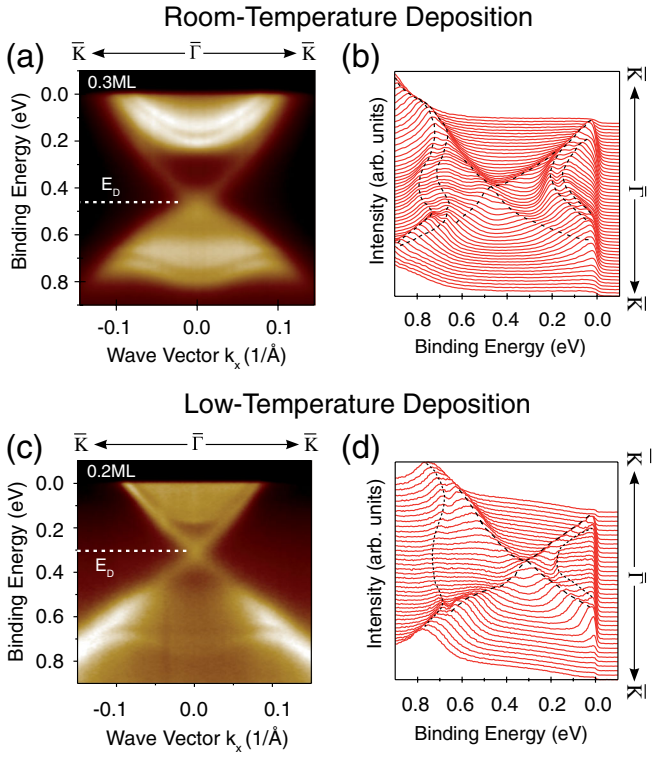

FIG. 2 (color online). Comparison of room-temperature and low-temperature deposition at the same measurement temperature of 8 K. Extra M-shaped bands in the valence-band range are seen to coexist with the Dirac point. The photon energy is 18 eV in (a),(b) and 21.5 eV in (c),(d).

Ref. [26]. The coexistence of the two M-shaped bands with an intact Dirac cone in the present study rules out the possibility that the upper M-shaped band is derived from the topological surface state, and, consequently, a gap cannot be assigned to these two features.

Third, the exposure of Bi_2Se_3 to nonmagnetic adsorbates has been tested recently, and CO adsorption revealed several M-shaped bands [30]. Their formation was assigned to a quantization of valence states in the direction perpendicular to the surface [30].

In Fig. 2(a), we observe near the Fermi energy a pair of well-resolved parabolas which are nested, i.e., not displaced in **k** space relative to each other. In the previous work, such features have also been seen but with a pronounced Rashba-type spin-orbit splitting Δk [26]. The Rashba splitting was, however, accompanied by an energy shift of the Dirac point of much more than the value of 150 meV where our Fe-induced doping saturates. Moreover, in a most recent work, extra states with Rashba splitting at the Fermi energy have been obtained by just exposing the surface of Bi_2Se_3 to residual gas [31]. Their formation has been explained as a two-dimensional electron gas at the surface of Bi_2Se_3 due to band bending as a result of the surface doping. For the present experiment, this means that it is especially important not to cross contaminate the surface by other species during the Fe deposition experiments. That the doping-induced shift of 150 meV is most likely entirely the effect of the Fe will become clear from the comparison to low-temperature deposition below.

The situation is indeed altered drastically when Fe is deposited on Bi_2Se_3 at low temperatures. We show in Fig. 3 $E(k)$ dispersions of the topological surface states in the same energy range as before for a sample as cleaved and for deposited masses of 0.2 ML [also in Figs. 2(c) and 2(d)] and 0.4 ML.

The photoemission signal of the topological surface state is reduced more strongly than for room temperature at the same Fe deposition. In addition, we observe a change in the relative intensities of bulk and surface states so that for an acceptable contrast we had to change the photon energy from 18 to 21.5 eV. The Dirac point has shifted to a slightly *lower* binding energy when going from clean Bi_2Se_3 to 0.2 ML Fe, and this trend of hole doping is confirmed by the second deposition step (0.4 ML in total). From a comparison of normal emission spectra in Fig. 3(d), the total shift can be quantified as 55 meV. Again, no gap opens at the Dirac point. In addition, we observe an increased linearity of the surface-state dispersion above and below the Dirac point. Interestingly, for *bulk doping* of Bi_2Se_3 with Fe, the Dirac point was also found to shift to lower binding energies, indicating hole doping [24]. Indeed, it is known that Cu in Bi_2Se_3, which also has recently been studied by angle-resolved photoemission

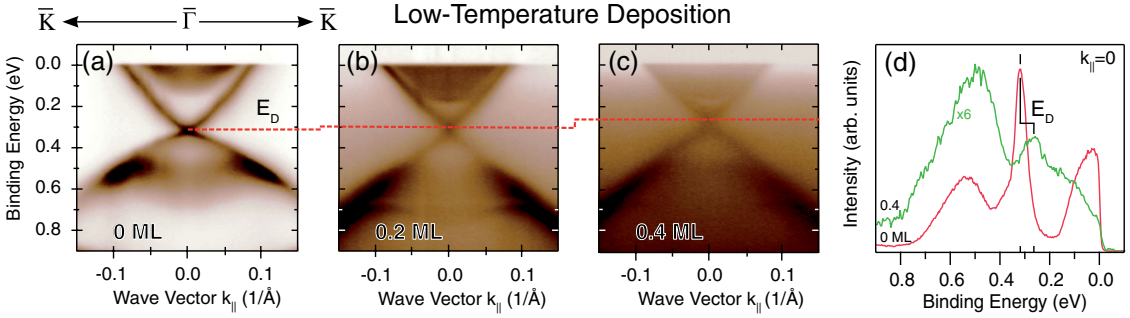

FIG. 3 (color online). Fe deposition at low temperature yields a shift of the Dirac point to lower binding energy (hole doping) and enhanced linearity in two subsequent deposition steps. Cleavage, Fe deposition, and measurement were done at 8 K. No gap appears in the topological surface state. The photon energy is 18 eV in (a) and 21.5 eV in (b),(c).

[32], can act as a donor or an acceptor depending on whether it resides at Bi sites (donor) or interstitial sites (acceptor) [33], so the different signs of the Fe doping at room temperature and low temperature likely correspond to different growth mechanisms of Fe on top of Bi_2Se_3. Regarding the bulk valence and conduction states, we find that these states appear to shift to a *higher* binding energy at low temperature, thus showing a behavior which contrasts with that of the topological surface state. In addition, a quantization similar to the deposition at room temperature is seen, especially for 0.2 ML in the valence band; see Fig. 2(d).

The different effects which room- and low-temperature deposition have on the surface doping of Bi_2Se_3 can be substantiated by core-level spectroscopy which is sensitive to the chemical environment. The first point is the spectroscopic confirmation of the Fe deposition. Fe3p falls energetically together with the Se3$d_{3/2}$ peak [Figs. 4(a) and 4(c)]. To demonstrate this, we plotted in the inset of Fig. 4(a) for comparison an Fe3p signal from a comparable deposition on a Bi_2Te_3 sample [34]. In fact, the Se3d core level is seen to grow upon Fe deposition in the binding energy range of the Fe3p, as uncovered by a fit

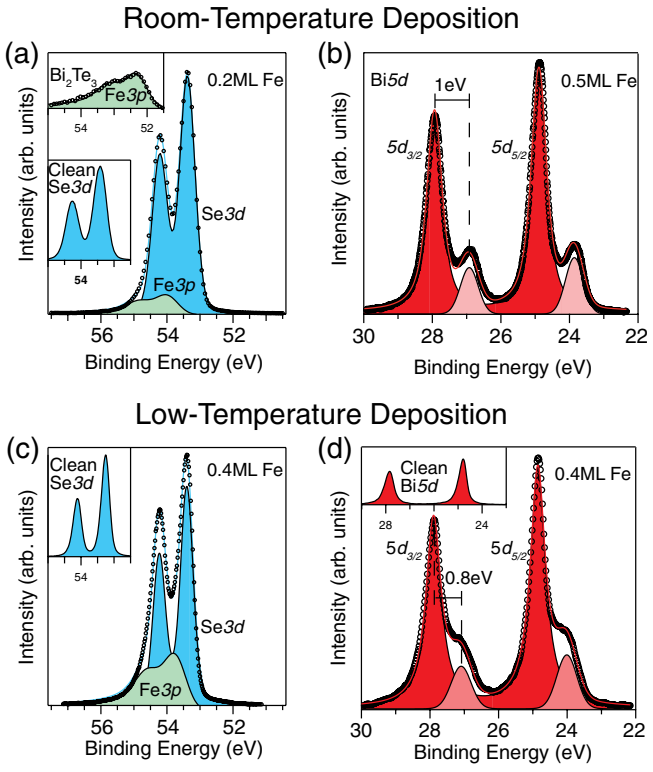

FIG. 4 (color online). Core-level spectroscopy distinguishes the different deposition methods. (a),(c) The Se3d core levels cover the Fe3p emission. Se3d shifts to higher binding energy only for low-temperature (8 K) deposition of the Fe. (b),(d) Bi5d develops shoulders with the core-level shifts having different values for room-temperature and low-temperature preparation. The photon energy is 125 eV, and temperatures were the same during deposition and measurement.

which takes into account the line shape from the pristine Se3d peak as well as that of Fe3p on Bi_2Te_3. The next questions are whether we observe a chemical interaction in Bi_2Se_3 due to the Fe and if there is a difference between room- and low-temperature deposition. Both can indeed be answered positively: The Fe deposition leads to a new structure in the Bi5d core level. This structure is shifted to lower binding energy and more so for room- than for low-temperature deposition. The data in Figs. 4(b) and 4(d) allow for a quantification of the shift as 1.0 and 0.8 eV, respectively. On the pure Bi_2Se_3 sample, the cooling alone has the effect of an overall shift to a higher binding energy but no shifted peak or shoulder appears which agrees with the physisorption picture of adsorbates and its observed reversibility when warming up again. The Se3d does not move during Fe deposition at room temperature but shows an overall shift to a higher binding energy when the Fe is deposited at low temperature.

These observations can be explained as follows. The stoichiometry of Bi_2Se_3 suggests to formally assign the Bi atoms a $3+$ oxidation state and the Se atoms a $2-$ state. Then, the shoulders of Bi5d would be assigned to Bi with a lower oxidation state than $3+$. The Se, instead, cannot take a lower oxidation state. The Fe, on the other hand, is expected to sit as individual atoms on top at low temperature but may be considerably more mobile at room temperature, forming possibly islands or even assuming subsurface sites. The reduced oxidation state of Bi5d would then follow from a newly formed Bi bond to Fe. The top layer of Bi_2Se_3 is known to be a Se layer [35], but, even in the on-top position on the Se layer, the Fe could cause the Bi5d shoulder if the new bonds between Fe and Se affect, i.e., weaken, the interlayer bonding between Se and Bi atoms.

This means that the fact that the two Fe deposition methods which show doping in opposite directions can very well be distinguished by different chemical environments. Such have been established also for magnetic impurities in bulk systems before; an example is Mn in the diluted ferromagnetic semiconductor $Ga_{1-x}Mn_xAs$, which is a double donor at interstitial sites and an acceptor at Ga sites [36]. In the present case, a photoelectron diffraction experiment would be timely to also clarify the electronically identified sites of the Fe structurally.

Finally, we want to note that it is quite surprising that the topological surface state is reported to open a band gap due to time-reversal symmetry breaking while the Rashba split states do not open any gap at their Kramers point. This further supports our conclusion that the gap in Ref. [26] is of extrinsic origin and not due to the deposited Fe impurities or their magnetism. If it was that easy to open a gap in the topological surface state by Fe impurities in the bulk without any ferromagnetic order [24] or submonolayer amounts of Fe at the surface [26], this would not be good news for constructing the proposed devices of ferromagnetic layers and topological insulators listed in the outset. The present results allow for the deposition of the

ferromagnetic material which then can be magnetized in various ways and ideally will control the transport properties of the topological insulator via its surface state. The simulation in Ref. [26] demonstrates that a band gap in the surface state requires a magnetization perpendicular to the surface. The topological surface state could mediate such magnetization when the Dirac point is near the Fermi energy [27], which is not the case with Fe/Bi_2Se_3 due to the strong n doping.

In conclusion, we find that the topological surface state of Bi_2Se_3 is tolerant against magnetic adsorbates. This indicates that topological insulators such as Bi_2Se_3 can be interfaced with a ferromagnet without losing the topological surface state and its unique quasirelativistic dispersion and Dirac point. Our results contradict magnetization as the origin of the gaplike feature reported before. In order to exhaust possible preparation conditions, room- and low-temperature deposition have been compared. They lead to very different behavior, i.e., an opposite doping trend and different chemical environments, but they agree in the dispersion of the topological surface state and its gapless nature. The presently found robustness is the precondition for the exploration and the successful functionalization of interfaces between topological insulators and ferromagnets. This will involve growing a perpendicularly magnetized ferromagnetic film on top of a topological insulator and monitoring the effect of the exchange coupling on the topological surface state underneath.

Note added in proof.—X-ray magnetic dichroism reveals that the magnetic anisotropy of Fe on Bi_2Se_3 is within the surface plane [37]. In agreement with the simulations of Ref. [26], no gap is expected for this configuration.

[1] C. L. Kane and E. J. Mele, Phys. Rev. Lett. **95**, 146802 (2005); **95**, 226801 (2005).
[2] Liang Fu and C. L. Kane, Phys. Rev. B **76**, 045302 (2007).
[3] B. A. Bernevig and S. C. Zhang, Phys. Rev. Lett. **96**, 106802 (2006).
[4] Liang Fu, C. L. Kane, and E. J. Mele, Phys. Rev. Lett. **98**, 106803 (2007).
[5] J. E. Moore and L. Balents, Phys. Rev. B **75**, 121306 (2007).
[6] R. Roy, Phys. Rev. B **79**, 195322 (2009).
[7] S. Murakami, New J. Phys. **9**, 356 (2007).
[8] M. König, S. Wiedmann, C. Brüne, A. Roth, H. Buhmann, L. W. Molenkamp, X.-L. Qi, and S.-C. Zhang, Science **318**, 766 (2007).
[9] X. L. Qi, T. L. Hughes, and S. C. Zhang, Nature Phys. **4**, 273 (2008).
[10] X. L. Qi, T. L. Hughes, and S. C. Zhang, Phys. Rev. B **78**, 195424 (2008).
[11] T. Yokoyama, Y. Tanaka, and N. Nagaosa, Phys. Rev. B **81**, 121401 (2010).
[12] I. Garate and M. Franz, Phys. Rev. Lett. **104**, 146802 (2010).
[13] S. Mondal, D. Sen, K. Sengupta, and R. Shankar, Phys. Rev. Lett. **104**, 046403 (2010).
[14] Zhenhua Wu, F. M. Peeters, and Kai Chang, Phys. Rev. B **82**, 115211 (2010).
[15] Ya Zhang and Feng Zhai, Appl. Phys. Lett. **96**, 172109 (2010).
[16] A. A. Burkov and D. G. Hawthorn, Phys. Rev. Lett. **105**, 066802 (2010).
[17] B. D. Kong, Y. G. Semenov, C. M. Krowne, and K. W. Kim, Appl. Phys. Lett. **98**, 243112 (2011).
[18] D. Hsieh, D. Qian, L. Wray, Y. Xia, Y. S. Hor, R. J. Cava, and M. Z. Hasan, Nature (London) **452**, 970 (2008).
[19] D. Hsieh, Y. Xia, D. Qian, L. Wray, J. H. Dil, F. Meier, J. Osterwalder, L. Patthey, J. G. Checkelsky, N. P. Ong, A. V. Fedorov, H. Lin, A. Bansil, D. Grauer, Y. S. Hor, R. J. Cava, and M. Z. Hasan, Nature (London) **460**, 1101 (2009).
[20] H. Zhang, C.-X. Liu, X.-L. Qi, Xi Dai, Z. Fang, and S.-C. Zhang, Nature Phys. **5**, 438 (2009).
[21] Y. L. Chen *et al.*, Science **325**, 178 (2009).
[22] M. R. Scholz, J. Sánchez-Barriga, D. Marchenko, A. Varykhalov, A. Volykhov, L. V. Yashina, and O. Rader, arXiv:1108.1053v2.
[23] Z.-H. Pan, E. Vescovo, A. V. Fedorov, D. Gardner, Y. S. Lee, S. Chu, G. D. Gu, and T. Valla, Phys. Rev. Lett. **106**, 257004 (2011).
[24] Y. L. Chen, J. H. Chu, J. G. Analytis, Z. K. Liu, K. Igarashi, H. H. Kuo, X. L. Qi, S. K. Mo, R. G. Moore, D. H. Lu, M. Hashimoto, T. Sasagawa, S. C. Zhang, I. R. Fisher, Z. Hussain, and Z. X. Shen, Science **329**, 659 (2010).
[25] Y. S. Hor, P. Roushan, H. Beidenkopf, J. Seo, D. Qu, J. G Checkelsky, L. A. Wray, D. Hsieh, Y. Xia, S.-Y Xu, D. Qian, M. Z. Hasan, N. P. Ong, A. Yazdani, and R. J. Cava, Phys. Rev. B **81**, 195203 (2010).
[26] L. A. Wray, S. Y. Xu, Y. Xia, D. Hsieh, A. V. Fedorov, Y. San Hor, R. J. Cava, A. Bansil, H. Lin, and M. Z. Hasan, Nature Phys. **7**, 32 (2010).
[27] Q. Liu, C.-X. Liu, C. Xu, X.-L. Qi, and S.-C. Zhang, Phys. Rev. Lett. **102**, 156603 (2009).
[28] D. A. Abanin and D. A. Pesin, Phys. Rev. Lett. **106**, 136802 (2011).
[29] R. R. Biswas and A. V. Balatsky. Phys. Rev. B **81**, 233405 (2010).
[30] M. Bianchi, R. C. Hatch, J. Mi, Bo Brummerstedt Iversen, and Ph. Hofmann, Phys. Rev. Lett. **107**, 086802 (2011).
[31] M. Bianchi, D. Guan, S. Bao, J. Mi, Bo Brummerstedt Iversen, Ph. D. C. King, and Ph. Hofmann, Nature Commun. **1**, 128 (2010).
[32] A. A. Kordyuk, T. K. Kim, V. B. Zabolotnyy, D. V. Evtushinsky, M. Bauch, C. Hess, B. Büchner, H. Berger, and S. V. Borisenko, Phys. Rev. B **83**, 081303 (2011).
[33] A. Vaško, L. Tichý, J. Horák, and J. Weissenstein, Appl. Phys. A **5**, 217 (1974).
[34] M. R. Scholz, J. Sánchez-Barriga, D. Marchenko, A. Varykhalov, A. Volykhov, L. V. Yashina, and O. Rader, arXiv:1108.1037.
[35] R. W. G. Wyckoff, *Crystal Structures* (Wiley, New York, 1964), Vol. 2.
[36] See, e.g., *Spintronics*, edited by T. Dietl, D. D. Awschalom, M. Kaminska, and H. Ohno (Elsevier, San Diego, CA, 2008).
[37] J. Honolka *et al.*, following Letter, Phys. Rev. Lett. **108**, 256811 (2012).